Two-Point Measurements of Post-shock Overpressure Past a Grid Turbulence

T. Harasaki, T. Kitamura, Akihiro Sasoh, K. Nagata, and Y. Sakai

1 Introduction

Interaction between a shock wave and turbulence can yield complementary impacts to each other; when a shock wave is attenuated in turbulence the turbulent flow can gain energy from the shock wave, and vice versa. Moreover, various dissipation processes may accompany and result in various phenomenological impacts, for example, emission of acoustic waves and attenuation or enhancement of sonic boom [1]-[4]. However, in spite of quite a few past works, quantitative characteristics and detailed mechanisms of the interaction between a shock wave and isotropic turbulence still warrant further investigations.

Lele formulated the shock-jump relations in a turbulent flow [5]. Xanthos et al. experimentally demonstrated that the fluctuation in the post-shock over pressure was amplified after the interaction with grid turbulence while the shock wave was attenuated in particular with a fine grid [6]. The impacts of isotropic turbulence on shock wave characteristics have been studied numerically, too. Lee et al. and Hasegawa & Noguchi showed deformation and smearing of a shock wave due to isotropic turbulence [7], [8]. Averiyanov et al. [9] modeled finite amplitude acoustic wave through atmospheric turbulence using Khokhlov-Zabolotskaya-Kuznetsov type equation, thereby demonstrating production of focusing and defocusing regions and evaluating statistical behavior, time-of-flight, peak pressure and rise time, of N-waves. However, experimental data of the same kind is far from sufficient.

The purpose of this study is to obtain experimental data to characterize the post-shock overpressure modulation after interaction between a shock wave and a grid turbulence which represents isotropic turbulence. In the present experiment, the primary interest is to evaluate the peak value of the post-shock overpressure. Note here that in this study the shock thickness, which determines the rise time of the

T. Harasaki · T. Kitamura · Akihiro Sasoh · K. Nagata · Y. Sakai
Graduate School of Engineering, Nagoya University, Furo-cho, Chikusa-ku,
Nagoya 464-8603, Japan

R. Bonazza and D. Ranjan (eds.), *29th International Symposium on Shock Waves 2*,
DOI: 10.1007/978-3-319-16838-8_97

post-shock overpressure, is too small to be resolved experimentally due to a finite size of the pressure transducers, thereby being out of the scope of this study. A blast-like shock wave is generated using an open-end, long and thin shock tube, and interacted with a grid turbulence generated in a low-turbulence wind tunnel.

2 Apparatus and Method

Turbulent flow was generated using a square grid in a low-turbulence wind tunnel. The length and the cross section of the wind tunnel test section were 4 m and 0.994 m $\times$ 0.46 m, respectively. A biplane grid with square mesh was set at the entrance, and location of the test cross-section of shock wave-turbulence interaction was 1.5 m downstream (Fig. 1). Over the test section, the distributions of a time-averaged flow speed, U_∞, was measured using an I-type hot-wire anemometer. Over Region A in the test cross-section, the spatial variation in U_∞, was less than $\pm$ 0.6 %. Three kinds of square grids of a solidity of 0.36 were examined. Each grid element rod had a d mm $\times$ d mm square cross-section, a mesh size of L mm.

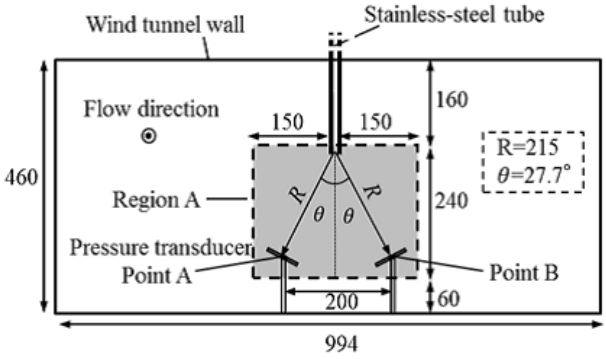

Fig. 1 Schemaic illustration of test section

A shock wave was ejected from a 5.4-mm-inner-dia., 3.75-m-long, stainless-steel tube, which was connected to a driver air reservoir using a quick-piston opening valve. In order to avoid water freezing, dry air was charged into the driver air reservoir. Along the stainless-steel tube, three piezoelectric pressure transducers (H113A21, PCB Piezotronics inc., 3.6 mV/kPa, rise time 1μs) were set to measure an in-tube shock Mach number. In this study, the overpressure histories measured at two points both with R = 215 mm and θ = 27.7 deg. (see Fig. 1) were employed; two aluminum flat plates, 130 mm (chord) $\times$ 50 mm (span) $\times$ 6 mm (thickness), were set normal to the propagation direction of the spherical wave; a piezoelectric pressure transducer was flush-mounted on each plate in order to measure the time-variation of the overpressure behind a reflected shock wave. Among

commercially-available products, a piezoelectric pressure transducer with acceleration compensation (113B28, PCB Piezotronics inc.) was chosen due to its short rise time, 1 μs, and high sensitivity, 14.5 mV/kPa. In order to suppress disturbances to the uniform flow, the flat plates had a 6-mm-dia. circular leading edge and a tapered tail. The horizontal separation distance between the pressure transducers in the transverse direction to the flow was 200 mm.

The system of shock wave generation, pressure measurement and recording was automatically run using a personal computer and solenoid valves. In all experiments, the fill pressure in the driver gas reservoir was set to 1.0 MPa (absolute value). Under each experimental condition presented hereafter, an ensemble average and a standard deviation were obtained after either 500 or 1000 runs.

3 Examples of Overpressure History

Figures 2 to 4 show examples of overpressure histories induced by a shock wave which are measured at Points A and B with the same time origin. Without a grid (Fig. 2), the overpressure histories, with respect both to the peak value, ΔP_{peak} and to the relative arrival time, coincide well with each other. However, with the grid in most of runs they differ to a sensible extent. For example, in Case 1 of Fig. 3, ΔP_{peak} at Point B is larger than that at Point A; the difference in arrival time at Point B relative to Point A, τ_{BA}, has a positive value. On the other hand, in Case 2 of Fig. 4, even under the same nominal run condition the relations become reversed; ΔP_{peak} at Point A is larger than that at Point B; τ_{BA} has a negative value. Such results almost randomly appear run by run. Their statistical behavior will be processed after 500 or 1000 runs under a same turbulence condition.

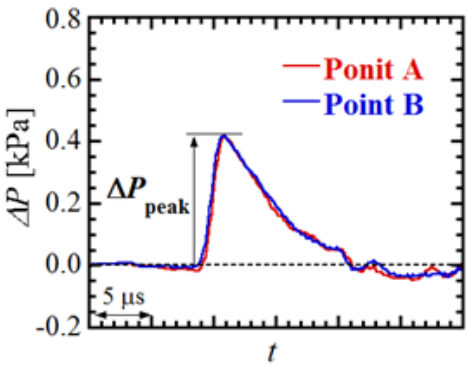

Fig. 2 Examples of overpressure histories, U_∞=20 m/s, without grid, $u' = 0.1$ m/s

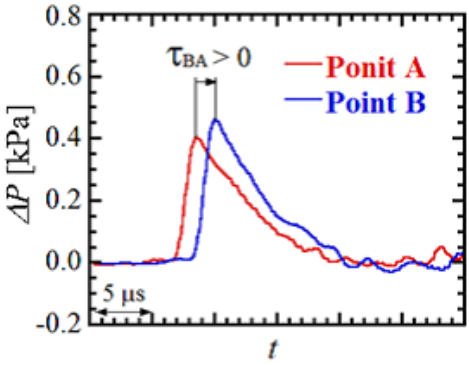

Fig. 3 Examples of overpressure histories, U_∞=20 m/s, with Grid-100, $u' = 1.2$ m/s, Case 1

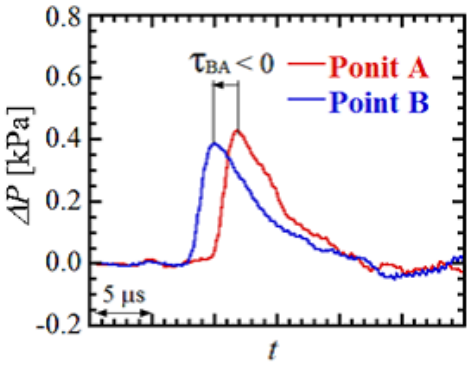

Fig. 4 Examples of overpressure histories, U_∞=20 m/s, with Grid-100, $u' = 1.2$ m/s

4 Correlation between Two Points

Figures 5 and 6 plot correlations with respect to peak overpressure and relative arrival time between Points A and B. Here, the normalized overpressure, $\tilde{\beta}$ is defined by

$$\tilde{\beta} \equiv \frac{\Delta P_{peak}}{P_\infty} \tag{1}$$

where P_∞ denotes an ambient pressure. As shown in Fig. 5, the overpressure modulations due to turbulence at Points A and B are almost independent of each other; the correlation coefficient with respect to β (=0.05) is much smaller than those without grid. In the cases without a gird, that is at a low turbulent intensity, the scatter in the strength of the shock wave were closely related to the scatter in the shock wave generator performance; the location of the measurement did not matter. However, with the much stronger velocity fluctuation, the correlation between the two

locations almost diminished although the scatter in the peak value became much larger. Here, a dimensionless arrival time difference, $\tilde{\tau}_{BA}$ is defined by

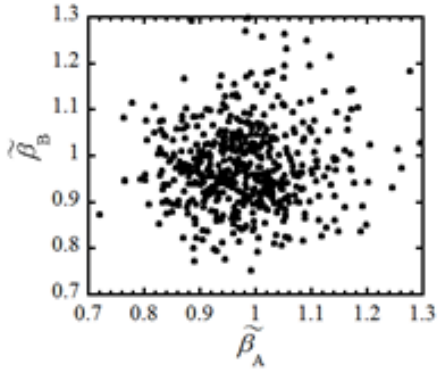

Fig. 5 Correlation between $\tilde{\beta}_A$ and $\tilde{\beta}_B$, U_∞=20 m/s, with Grid-100, $u' = 1.2$ m/s,, C=0.05

As seen in Fig. 6, with the grid the correlation coefficient, $C(\tilde{\beta}_B - \tilde{\beta}_A, \tilde{\tau}_{BA})$ has a positive value, being almost constant of about 0.25. On the other hand, the correlation coefficient almost vanishes without grid. This tendency can be explained that when the flow in front of the shock wave has an incoming velocity the relative shock Mach number and then the post-shock pressure are increased, while the arrival of the shock wave is delayed. On the other hand, if the flow has the opposite velocity sign, the shock Mach number and then the post-shock overpressure are decreased; the arrival becomes earlier.

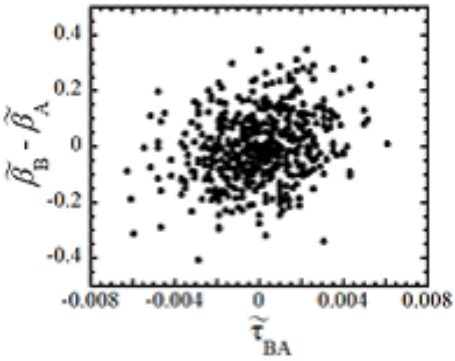

Fig. 6 Correlation between $\tilde{\tau}_{BA}$ and $\tilde{\beta}_A - \tilde{\beta}_B$, U_∞=20 m/s, with Grid-100, $u' = 1.2$ m/s,, C=0.25

5 Conclusion

It is confirmed that the peak overpressure measured at the two points, apart by 5 to 15 times as large as the turbulence integral scale are almost independent (C=0.05). However, a positive correlation coefficient (C=0.25) was obtained between the difference in peak value of the post-shock overpressure and that in the shock wave arrival time, which was caused by the variation of the relative shock Mach number to the upstream flow.

Acknowledgements. The authors would like to express our gratitude to Messrs. Katsuyoshi Kumazawa and Takao Sumi, Technical Division, and Dr. Shigeru Yokota and Mr. Hiroki Saito, all with Nagoya University for their valuable technical assistances. Also, we appreciate technical assistances from Mr. Kakuei Suzuki in numerically processing overpressure signals. This research was supported by Japan Aerospace Exploration Agency as a project No. 27-J-J6711 and as Grant-in-Aid for Scientific Research (S) 22226014 from Japan Society for the Promotion of Science.

References

1. Bass, H.E., Layton, B.A., Bolen, L.N., Raspet, R.: Propagation of medium strength shock waves through the atmosphere. J. Acoust. Soc. Am. 82(1), 306–310 (1987)
2. Raspet, R., Bass, H.E., Yao, L., Boulanger, P., McBride, W.E.: Statistical and numerical study of the relationship between turbulence and sonic boom characteristics. J. Acoust. Soc. Am. 96(6), 3621–3626 (1994)
3. Boulanger, P., Raspet, R., Bass, H.E.: Sonic boom propagation through a realistic turbulent atmosphere. J. Acoust. Soc. Am. 98(6), 3412–3417 (1995)
4. Lee, R.A., Downing, J.M.: Comparison of measured and predicted lateral distribution of sonic boom overpressures from the United States Air Force sonic boom database. J. Acoust. Soc. Am. 99(2), 768–776 (1996)
5. Lele, S.K.: Shock-jump relations in a turbulent flow. Phys. Fluids A. 4(12), 2900–2905 (1992)
6. Xanthos, S., Briassulis, G., Andreopoulos, Y.: Interaction of decaying freestream turbulence with a moving shock wave: pressure field. J. Propul. Power. 18(6), 1289–1297 (2002)
7. Lee, S., Lele, S., Moin, P.: Direct numerical simulation of isotropic turbulence interacting with a weak shock wave. J. Fluid Mech. 251, 533–562 (1993)
8. Hasegawa, T., Noguchi, S.: Numerical study of a turbulent flow compressed by a weak shock wave. Int. J. Comput. Fluid Dynamics 8(1), 63–75 (1997)
9. Averiyanov, M., Blanc-Benon, P., Cleveland, R.O., Khokhlova, V.: Nonlinear and diffraction effects in propagation of N-waves in randomly inhomogeneous moving media. J. Acous. Soc. Am. 129(4), 1760 (2011)